Shear Banding in an F-Actin Solution

Itsuki Kunita,[1] Katsuhiko Sato,[2] Yoshimi Tanaka,[3] Yoshinori Takikawa,[4] Hiroshi Orihara,[4] and Toshiyuki Nakagaki[1,5,*]

[1]*Department of Complex and Intelligent Systems, Faculty of Systems Information Science, Future University Hakodate, Kameda-nakano 116-2, Hakodate 041-8655, Japan*
[2]*RIKEN Center for Developmental Biology, Minatojima Minami 2-2-3, Kobe 650-0047, Japan*
[3]*Department of Mechanical Engineering and Material Science, Yokohama National University, Tokiwadai 79-5, Hodogaya, Yokohama 240-8501, Japan*
[4]*Division of Applied Physics, Faculty of Engineering, Hokkaido University, N13W8, Sapporo 060-8628, Japan*
[5]*JST, CREST, 5, Sanbancho, Chiyoda-ku, Tokyo 102-0075, Japan*

(Received 4 August 2012; published 10 December 2012)

We report herein the first evidence that an F-actin solution shows *shear banding*, which is characterized by the spontaneous separation of homogeneous shear flow into two macroscopic domains of different definite shear rates. The constant shear stress observed in the F-actin solution is explained by the banded flow with volume fractions that obey the lever rule. Nonhomogenous reversible flows were observed in the F-actin solution with respect to upward and downward changes in the shear rate. This is the first time shear banding has been observed in a simple biomacromolecule. The biological implications and dynamic aspects of shear flow velocity characteristic patterns are discussed.

DOI: 10.1103/PhysRevLett.109.248303 PACS numbers: 83.60.Df, 83.50.Ax, 87.19.rh, 82.35.Pq

Introduction.—Biomacromolecules are of great interest because they are closely related to the physiological functions in a cell. One such biomacromolecule, actin, is one of the most abundant proteins in eukaryotic cells and is a major component of the cytoskeleton, cortex, and protoplasm; in a sense, cells are actin solutions [1].

Actin molecules assemble in aqueous solutions to form long filamentous structures (F-actin) [2]. These rodlike molecules form temporal network structures even at low concentrations, and show nonlinear rheological responses. Investigation into the rheological behavior of actin solutions [3] is essential to understand the flow, deformation, and transport properties of the protoplasm, which are closely related to functions such as its motility, morphology, and cytokinetics.

In 1974 Maruyama *et al.* precisely measured the viscosity of purified F-actin solution as a function of shear rate $\dot{\gamma}$, and found that the viscosity was inversely proportional to $\dot{\gamma}$ in the range $0.0005 \leq \dot{\gamma} \leq 5.0\ \mathrm{s}^{-1}$ [4]. This result indicates that shear stress (given by shear rate $\times$ the viscosity) is constant in the shear rate range. This finding was confirmed by other investigators [5], and is referred to as *indeterminate fluid* behavior because the shear rate cannot be uniquely determined at constant stress. The origin and mechanism of the behavior of F-actin solutions remains unclear.

However, if we turn our attention to the field of complex fluids such as polymer and surfactant solutions, several systems exhibit constant shear stress [6,7], which is referred to as the *stress plateau*. The best-investigated examples of such systems are surfactant solutions of cetylpyridinium chloride or cetyltrimethylammonium bromide, in which surfactants aggregate to form long cylindrical structures, wormlike micelles. In these solutions the appearance of the stress plateau is recognized as a consequence of shear-induced phase transition, *shear banding*.

Shear banding is a phenomenon in which the homogeneous shear flow spontaneously separates into two macroscopic domains (bands) of different definite shear rates, $\dot{\gamma}_1$ and $\dot{\gamma}_2$ ($\dot{\gamma}_1 < \dot{\gamma}_2$). These two domains have a common shear stress σ as $\sigma = \eta_1\dot{\gamma}_1 = \eta_2\dot{\gamma}_2$, where η_1 and η_2 are constant viscosities of the two domains, respectively ($\eta_1 > \eta_2$). If the applied shear rate $\bar{\dot{\gamma}}$ (given by the relative speed of the two plates in the rheometer divided by the distance between the plates) varies in the range of $\dot{\gamma}_1 < \bar{\dot{\gamma}} < \dot{\gamma}_2$, and the volume fractions of the two domains satisfy the relation, called the *lever rule*

$$\bar{\dot{\gamma}} = (1 - \phi)\dot{\gamma}_1 + \phi\dot{\gamma}_2, \tag{1}$$

where ϕ is the volume fraction of the domain with the shear rate $\dot{\gamma}_2$, the shear stress turns out to be constant in $\dot{\gamma}_1 < \bar{\dot{\gamma}} < \dot{\gamma}_2$. This is the shear banding scenario [8] and its validity has been checked by various experimental techniques such as NMR and birefringence [9–11].

In addition, the mesostructural or microstructural change in the solution is thought to be the mechanism behind shear banding in complex fluids. For example, in the case of the surfactant solutions (cetylpyridinium chloride and cetyltrimethylammonium bromide), wormlike micelles entangle each other and form a network. The network and the wormlike micelles themselves are stochastically broken and reconstructed at equilibrium with some relaxation time, denoted by τ_R. The time τ_R is related to those times of the disentanglement (reptation) and

breakage of the micelles [8]. When the applied shear rate is lower than the characteristic shear rate $1/\tau_R$ ($\simeq \dot{\gamma}_1$), the system is homogeneous and its viscosity is high. However, when the applied shear rate exceeds the characteristic shear rate $1/\tau_R$, the microscopic structure begins to break and align in a particular direction determined by the flow. In general, breakage and orientation of the filamentous structures reduce their viscosity, so that high and low shear rate domains can coexist at applied shear rates beyond $\dot{\gamma}_1$.

Given that F-actin is also a reversible filamentous structure [12] and that its network structure is affected by the shear flow, it is reasonable to expect that the origin of the indeterminate fluid behavior observed in F-actin solutions is a banded flow whose volume fractions obey the lever rule, Eq. (1).

Here, to address this expectation, we carried out direct observations of the flow profile in the F-actin solution under simple shear flow using the particle image velocimetry (PIV) [13,14]. Last, we discuss the biological meanings and functions of shear banding in actin solutions, referring to the plug flow observed in the slime mold *Physarum polycephalum* [15] and in other amoeba [16].

Preparation of F-actin solution.—Crude globular actin (G-actin) was extracted from acetone powder of chicken breast muscle. The G-actin was purified according to the method of Spudich and Watt [17] and dissolved in G-buffer (1 mM $NaHCO_3$ (pH8.0), 2.0 mM ATP, 2.0 mM $CaCl_2$, 0.1 mM DTT) at 4 °C. KCl is a regulation factor of G-actin polymerization, so that the final concentration of KCl was set on 0.1 M in G-buffer [4]. The actin concentration in the solutions was 0.6 mg/ml. The G-actin concentration was determined by the Bradford method using bovine serum albumin as a standard protein.

Measurements of shear stress and flow velocity profile.—Rheological measurements were made using a cone-plate rheometer (MCR301, Anton Paar) with diameter of 50 mm. We also performed PIV measurements to obtain flow velocity profiles under shear flow. To achieve this, the bottom plate of the rheometer was replaced by a thin glass plate, through which carboxylate-modified fluorescence beads (1 μm in diameter, FluoSpheres F8823, invitrogen) dispersed in F-actin solutions were observed with a confocal scanning laser microscope (CSLM) (IX71, Olympus and CSU22, Yokogawa), as shown in Fig. 1(a). The observations were taken 5.7 mm from the center of the upper rotating plate, where the gap was 94 μm. The focal plane or the objective lens was periodically moved up and down by a piezoactuator (P-721.10, PI) attached to a water-immersion objective lens (40 ×). A triangular voltage of 2.5 Hz was applied to the piezoactuator so that the focal plane oscillated vertically with a span of 130 μm covering the gap, as shown in Fig. 1(b). Two hundred images (200 × 200 μm) were captured per oscillation period of (0.4 s). In a steady state, we calculated the average displacement of particles during a period at each height from the cross correlation between two time-successive images. The velocity obtained from the displacement was further averaged over five periods.

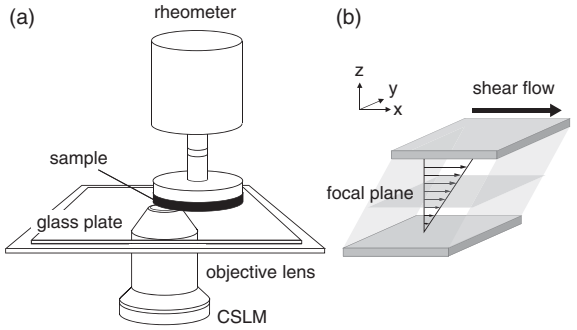

FIG. 1. (a) Schematic illustration of the system combining a rheometer and CSLM. (b) Schematic geometry of the observation region. Observation images were captured vertically every 1.3 μm.

Figure 2 shows several images of fluorescent beads for consecutive planes in a stack obtained at 1.00 s^{-1}. Image (a) covers all of the observed region (200 × 200 μm) in the plane located at $z = 45$ μm. We made the bead concentration (0.004 vol %) as low as possible so that the beads would not affect the rheological property of the F-actin solution. Images (b1)–(b6) show different planes of the same enclosed area as in image (a). The height difference between the consecutive images is 1.3 μm. One bead is

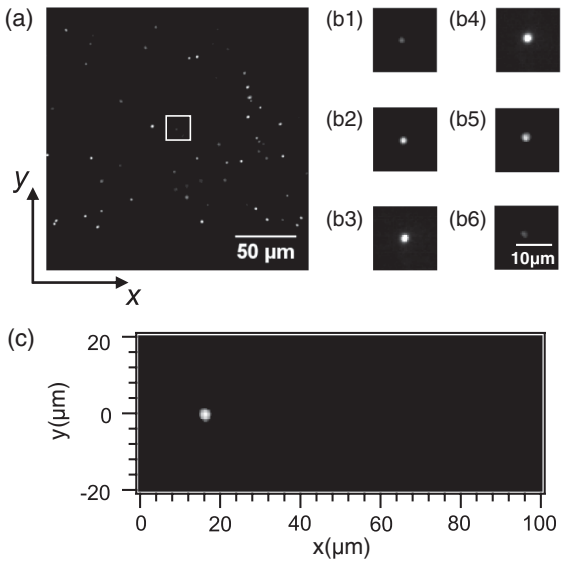

FIG. 2. Measurements of flow velocity profile. (a),(b) Several images of fluorescence beads for consecutive planes in a stack obtained at 1.00 s^{-1}. Image (a) is the full image of the observed area (200 × 200 μm), and images (b1)–(b6) are the same enclosed area as in image (a). Image (a) is located at $z = 45$ μm, and the height of the other images increases from (b1) to (b6) by 1.3 μm. (c) Cross correlation between two time-successive images at $z = 45$ μm, according to PIV measurement.

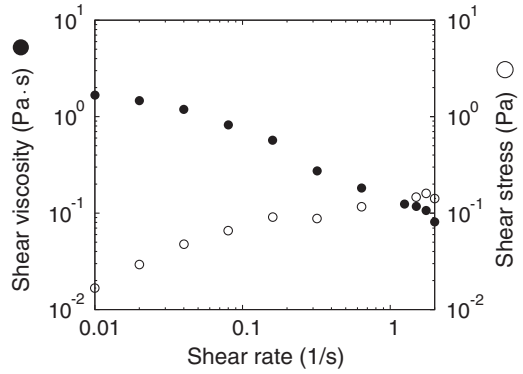

FIG. 3. Dependency of the shear stress and viscosity of F-actin solution with respect to upward changes in shear rate from 0.01 to 2.00 s^{-1}.

clearly observed in the area in images (b2)–(b5), indicating that the vertical resolution is about 5 μm. According to the PIV method, the cross correlation between two time-successive images at $z = 45$ μm is shown in Fig. 2(c). There is one sharp peak, which certifies sample homogeneity.

Rheological behavior of the bulk solution.—Figure 3 shows the dependency of shear stress and viscosity with respect to stepwise upward changes in applied shear rate $\bar{\dot{\gamma}}$ from 0.01 to 2.00 s^{-1}. The shear stress and viscosity on each step of $\bar{\dot{\gamma}}$ were measured repeatedly every second for 15 min. This time interval of 15 min was long enough for the system to attain the steady state. The data point on the figure indicates the mean average value over the 15 min of each step. The viscosity showed a tendency of shear thinning, and was roughly proportional to (shear rate)$^{-1}$ so that the shear stress was approximately constant. We observed that in the range of $\bar{\dot{\gamma}}$ from 0.08 to 2.00 s^{-1}, the slope of the stress-shear rate relation was smaller than that of lower region from 0.01 to 0.08 s^{-1}. In a higher region from 2.00 to 100 s^{-1}, the stress was increased more rapidly (data not shown). This result is consistent with a previous study [4], although the absolute values of physical parameters were different. Hereafter, we call the region of the stress-shear rate relation for the intermediate $\bar{\dot{\gamma}}$ (0.08–1.50 s^{-1}) the *stress plateau*.

Shear banding in the region of stress plateau.—Figure 4 shows the profiles of flow velocity measured along the gradient direction (z position) of shear rate applied between two plates. After 12 min from the beginning of each shear rate $\bar{\dot{\gamma}}$, the flow velocity was measured for 1 s and the measurement was repeated 5 times. Each data point in Fig. 4 was a mean value of the 5 repeats. Nonhomogeneous flows composed of high and low shear rate regions were observed at applied shear rates of 0.16 to 1.50 s^{-1}. For example, at 0.64 s^{-1} the low shear rate region extended from 20 to 70 μm of the z position, while two high shear rate regions extended from 0 to 20 μm and 70 to 90 μm. Figure 5 shows the dependency of the low

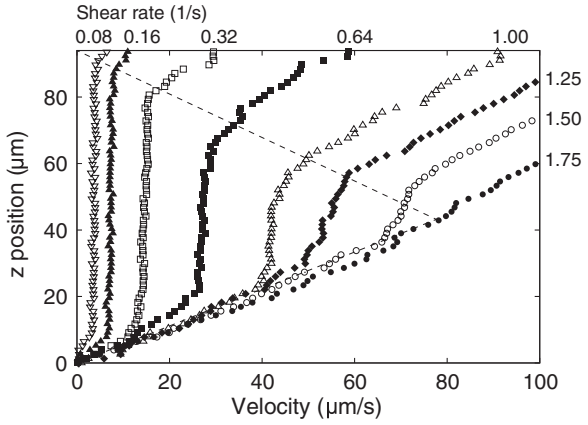

FIG. 4. Profiles of flow velocity measured along the gradient direction (z position) of the shear rate applied between two plates, at various shear rates from 0.08 to 1.75 s^{-1}. While the shear rate in the low shear rate region slightly increased with the applied shear rate, we can clearly distinguish the low and high shear rate regions.

shear rate region width on shear rates. The bandwidth decreased in proportion to the applied shear rate, and clear proportionality was observed. The region of shear rate in which banded flows was observed coincides with the region in which stress plateau appeared in the stress-shear rate curve.

Nonhomogenous reversible flows were observed in the F-actin solution with respect to downward changes in the shear rate, i.e., the velocity profiles did not show the flow history.

Since the nonhomogeneous flow appeared at $\bar{\dot{\gamma}} = 0.08$ s^{-1} and disappeared at $\bar{\dot{\gamma}} = 1.75$ s^{-1}, we could estimate $\dot{\gamma}_1$ and $\dot{\gamma}_2$ defined in Eq. (1) as $\dot{\gamma}_1 < 0.08$ s^{-1} and $\dot{\gamma}_2 = 1.75$ s^{-1}. More explicitly, we estimated $\dot{\gamma}_1$ as $\dot{\gamma}_1 = 0.0075$ s^{-1} from a least-squares fit to the low shear rate domain at $\bar{\dot{\gamma}} = 0.08$ s^{-1} in Fig. 4. With these values of $\dot{\gamma}_1$ and $\dot{\gamma}_2$ and according to the lever rule Eq. (1) we drew the dashed lines in Fig. 4. Obviously, these dashed lines were in good agreement with the boundaries between the

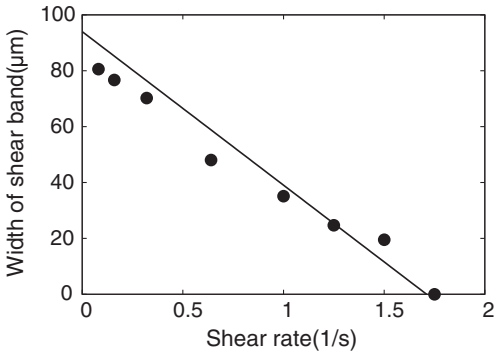

FIG. 5. Linear dependence of width of the low shear rate region on the applied shear rates.

low and high regions of the velocity profiled obtained in the experiments.

Conclusion and discussion.—We observed the velocity profiles of an F-actin solution under shear flow using the PIV technique and showed nonhomogeneous flows in the direction of the velocity gradient. The changes in volume fractions of the banded flow that satisfy the lever rule explain the stress plateau of the F-actin solution.

After the initial observation of F-actin solution constant shear stress by Maruyama *et al.* [4], some investigators suggested that solution nonhomogeneity may be a key to understanding the indeterminate fluid [18,19]. For example, Kerst *et al.* revealed the existence of ''polycrystalline domains'' of actin filaments at relatively high actin concentrations (> 6 mg/ml) using birefringence experiments [18].

While nonhomogeneous flow of the F-actin solution was demonstrated more directly in the present study, the microstructural or mesostructural states of the actin filaments at each domain (high and low shear rate regions) remain unknown. Several questions also remain to be answered, including whether the actin filament network breaks in the high shear rate regions, and if the actin molecular densities are the same in each domain. Since the mean length and persistence length of actin filaments are of the order of μm [20], the mesostructure of F-actin under flow is likely to be easy to investigate.

Cates *et al.* [8] stated that the characteristic relaxation time of the wormlike micelles, τ_R, is related to when the characteristic shear rate, $\dot{\gamma}_1$, at the onset of shear banding is $\dot{\gamma}_1 \simeq 1/\tau_R$. This prediction was confirmed in several experiments on the surfactant solutions [6]. If the origin and mechanism of F-actin shear banding are the same as those of surfactant solutions, the same relationship is expected to hold. Here, since nonhomogeneous flows appeared within 2 min of the shear rate being changed, we can estimate the relaxation time of F-actin solutions to be several tens of seconds. If we assume the τ_R of F-actin solutions is 10–100 s, then the characteristic shear rate is 0.01–0.1 s^{-1}. This approximately corresponds to the experimental value, suggesting that the origin and mechanism of F-actin shear banding are similar to those of surfactant solutions.

We discuss the biological implication of shear banding in an F-actin solution. The shear rate for shear banding was 0.1–1.5 s^{-1}, which corresponds to the speed of pseudopod extension and cell migration in some relatively large amoebas like true slime molds such as *Physarum polycephalum* and *Amoeba proteus*. The pseudopod is a local protrusion of the cell body that is pushed by protoplasmic flow from within, in a form of extension that is nonhomogeneous in space. As this also represents instability of homogeneous flow, the rheological property may play a role in amoeboid movement.

P. polycephalum and *A. proteus* contain intracellular channels through which the protoplasmic flow is faster than in the vicinity. This represents another instability of homogeneous flow and may also result from the rheological property. Thus, it is plausible that the occurrence of shear banding is closely related to the control of cell behaviors.

This research was supported by Strategic Japanese-Swedish Research Cooperative Program. I. K. and K. S. contributed equally to this work.

*nakagaki@fun.ac.jp

[1] D. Bray, *Cell Movements* (Garland, New York, 2001).
[2] B. Alberts *et al.*, *Molecular Biology of the Cell* (Garland Science, New York, 2008).
[3] P. A. Janmey, S. Hvidt, J. Peetermans, J. Lamb, J. D. Ferry, and T. P. Stossel, Biochemistry **27**, 8218 (1988).
[4] K. Maruyama, M. Kaibara, and E. Fukuda, Biochim. Biophys. Acta **371**, 20 (1974).
[5] R. E. Buxbaum, T. Dennerll, S. Weiss, and S. R. Heidemann, Science **235**, 1511 (1987).
[6] J. F. Berret, in *Molecular Gels*, edited by R. G. Weiss and P. Terech (Springer, Dordrecht, 2006), Chap. 19.
[7] S. Manneville, Rheol. Acta **47**, 301 (2008).
[8] N. A. Spenley, M. E. Cates, and T. C. B. McLeish, Phys. Rev. Lett. **71**, 939 (1993).
[9] P. T. Callaghan, M. E. Cates, C. J. Rofe, and J. B. A. F. Smeulders, J. Phys. II (France) **6**, 375 (1996).
[10] M. M. Britton, R. W. Mair, R. K. Lambert, and P. T. Callaghan, J. Rheol. **43**, 897 (1999).
[11] J. P. Decruppe, R. Cressely, R. Makhloufi, and E. Cappelaere, Colloid Polym. Sci. **273**, 346 (1995).
[12] M. Kasai, S. Asakura, and F. Oosawa, Biochim. Biophys. Acta **57**, 13 (1962).
[13] F. Arturo, J. Perez-Gonzalez, L. de Vargas, J. Rafael Castrejon-Pita, A. A. Castrejon-Pita, and G. Huelsz, J. Rheol. **47**, 1455 (2003).
[14] Y. T. Hu and A. Lips, J. Rheol. **49**, 1001 (2005).
[15] N. Kamiya, Cytologia **15**, 183 (1950).
[16] R. D. Allen, W. R. Pitts, D. Speir, Jr., and J. Brault, Science **142**, 1485 (1963).
[17] J. A. Spudich and S. Watt, J. Biol. Chem. **246**, 4866 (1971).
[18] A. Kerst, C. Chmielewski, C. Livesay, R. E. Buxbaum, and S. R. Heidemann, Proc. Natl. Acad. Sci. U.S.A. **87**, 4241 (1990).
[19] P. A. Janmey, S. Hvidt, J. Peetermans, J. Lamb, J. D. Ferry, and T. P. Stossel, Biochemistry **27**, 8218 (1988).
[20] A. Ott, M. Magnasco, A. Simon, and A. Libchaber, Phys. Rev. E **48**, R1642 (1993).